Eur. Phys. J. C 26, 51–66 (2002)
Digital Object Identifier (DOI) 10.1140/epjc/s2002-01036-y

THE EUROPEAN PHYSICAL JOURNAL C

The contribution of off-shell gluons to the structure functions F_2^c and F_L^c and the unintegrated gluon distributions

A.V. Kotikov[1,a], A.V. Lipatov[2], G. Parente[3,b], N.P. Zotov[4]

[1] Bogoliubov Laboratory of Theoretical Physics, Joint Institute for Nuclear Research, 141980 Dubna, Russia
[2] Department of Physics, M.V. Lomonosov Moscow State University, 119899 Moscow, Russia
[3] Departamento de Física de Partículas, Universidade de Santiago de Compostela, 15706 Santiago de Compostela, Spain
[4] D.V. Skobeltsyn Institute of Nuclear Physics, M.V. Lomonosov Moscow State University, 119899 Moscow, Russia

Received: 18 April 2002 / Revised version: 24 July 2002 /
Published online: 7 October 2002 –

Abstract. We calculate the perturbative parts of the structure functions F_2^c and F_L^c for a gluon target having non-zero transverse momentum squared at order α_s. The results of the double convolution (with respect to the Bjorken variable x_B and the transverse momentum) of the perturbative part and the unintegrated gluon densities are compared with the HERA experimental data for F_2^c. The contribution from the F_L^c structure function ranges in 10–30% of that of F_2^c at the kinematical range of the HERA experiments.

1 Introduction

Recently there have become available important new data on the charm structure function (SF), F_2^c, of the proton from the H1 [1,4] and ZEUS [2,3] Collaborations at HERA, which have probed the small-x_B region down to $x_B = 8 \times 10^{-4}$ and $x_B = 2 \times 10^{-4}$, respectively. At these values of x_B, the charm contribution to the total proton SF, F_2, is found to be around 25%, which is a considerably larger fraction than that found by the European Muon Collaboration at CERN [5] at larger x_B, where it was only $\sim 1\%$ of F_2. Extensive theoretical analyses in recent years have generally served to confirm that the F_2^c data can be described through the perturbative generation of charm within QCD (see, for example, the review in [6] and references therein).

In the framework of DGLAP dynamics [7,8] there are two basic methods to study heavy flavor physics. One of them [9] is based on the massless evolution of the parton distributions and the other [10] on the boson–gluon fusion process. There are also interpolating schemes (see [11] and references therein). The present HERA data [1–4] for the charm SF F_2^c are in good agreement with the predictions from [10].

We note, however, that perhaps more relevant analyses of the HERA data, where the x_B values are quite small, are those based on BFKL dynamics [12] (see discussions in the review of [13] and references therein), because the leading $\ln(1/x_B)$ contributions are summed. The basic dynamical quantity in the BFKL approach is the unintegrated gluon distribution $\Phi(x_B, k_\perp^2)$ (f_g is the (integrated) gluon distribution multiplied by x_B and $k_\perp$ is the transverse momentum)

$$f_g(x_B, Q^2) = \int^{Q^2} \mathrm{d}k_\perp^2 \Phi(x_B, k_\perp^2)$$
$$\text{(hereafter} \quad q^2 = -Q^2, \quad k^2 = -k_\perp^2), \qquad (1)$$

which satisfies the BFKL equation.

We define the Bjorken variables

$$x_B = Q^2/(2pq) \quad \text{and} \quad x = Q^2/(2kq) \qquad (2)$$

for lepton–hadron and lepton–parton scattering, respectively, where p^μ and k^μ are the hadron and the gluon 4-momenta, respectively, and q^μ is the photon 4-momentum.

Notice that the integral is divergent at the lower limit and this leads to the necessity to consider the difference $f_g(x_B, Q^2) - f_g(x_B, Q_0^2)$ with some non-zero Q_0^2 (see the discussions in Sect. 3), i.e.

$$f_g(x_B, Q^2) = f_g(x_B, Q_0^2) + \int_{Q_0^2}^{Q^2} \mathrm{d}k_\perp^2 \Phi(x_B, k_\perp^2). \qquad (3)$$

In our analysis below we will not use the Sudakov decomposition, which is sometimes quite convenient in high-energy calculations. However, it is useful to have relations between our calculations and the results in which the Sudakov decomposition has been used. The corresponding analysis will be done in the next section. Here we only note that the property $k^2 = -k_\perp^2$ (see (1)) comes from the fact that the Bjorken parton variables x_B in the standard and in the Sudakov approaches coincide.

[a] e-mail: kotikov@sunse.jinr.ru
[b] e-mail: gonzalo@fpaxp1.usc.es

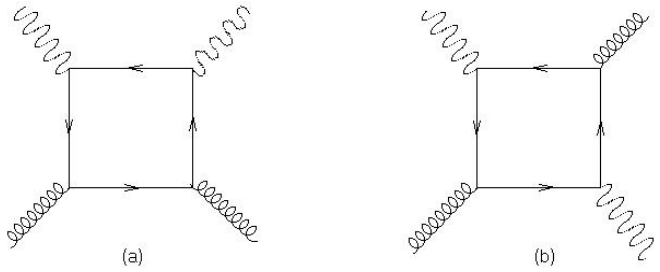

Fig. 1a,b. The diagrams contributing to $T_{\mu\nu}$ for a gluon target. They should be multiplied by a factor of 2 because of the opposite direction of the fermion loop. The diagram **a** should also be doubled because of the crossing symmetry

Then, in the BFKL approach the SFs $F^c_{2,\mathrm{L}}(x_\mathrm{B},Q^2)$ are driven at small x_B by gluons and are related in the following way to the unintegrated distribution $\Phi(x_\mathrm{B},k_\perp^2)$:

$$F^c_{2,\mathrm{L}}(x_\mathrm{B},Q^2) = \int_{x_\mathrm{B}}^1 \frac{\mathrm{d}x}{x}\int \mathrm{d}k_\perp^2 C^g_{2,\mathrm{L}}(x,Q^2,m_c^2,k_\perp^2)\Phi(x_\mathrm{B}/x,k_\perp^2), \quad (4)$$

The functions $C^g_{2,\mathrm{L}}(x_\mathrm{B},Q^2,m_c^2,k_\perp^2)$ may be regarded as the structure functions of the off-shell gluons with virtuality $k_\perp^2$ (hereafter we call them *hard structure functions*[1]). They are described by the quark box (and crossed box) diagram contribution to the photon–gluon interaction (see Fig. 1).

The purpose of this article is to calculate these hard SF $C^g_{2,\mathrm{L}}(x_\mathrm{B},Q^2,m_c^2,k_\perp^2)$ and to analyze the experimental data for $F_2^c(x_\mathrm{B},Q^2)$ by applying (4) with different sets of unintegrated gluon densities (see [18,17]) and to give predictions for the longitudinal SF $F_\mathrm{L}^c(x_\mathrm{B},Q^2)$.

It is instructive to note that the diagrams shown in Fig. 1. are similar to those of the photon–photon scattering process. The corresponding QED contributions have been calculated many years ago in [19] (see also the beautiful review in [20]). Our results have been calculated independently and they are in full agreement with [19] (see Appendix B). However, we hope that our formulas, which are given in a more simple form, could be useful for other authors.

The structure of this article is as follows: in Sect. 2 we present the basic formalism of our approach with a brief review of the calculational steps (based on [21]). The connection of our analysis with the Sudakov-like approach is also given. Later, we present the results for the two most important polarization matrices for off-shell gluons into the proton. In Sect. 3 and 4 we give the predictions for the structure functions F_2^c and F_L^c for the two cases of the unintegrated gluon distribution functions (see [18,17]) used, which are shortly reviewed. In Appendix A we show the basic technique for the evaluation of the required Feynman diagrams. Appendix B contains the review of QED results from [19,20]. In Appendix C we consider the limiting cases, when the values of the quark mass or the gluon momentum are equal to zero and also when the value of the photon "mass" Q^2 goes to zero.

2 Approach

The hadron part of the deep inelastic (DIS) spin-average lepton–hadron cross-section can be represented in the form[2]

$$F_{\mu\nu} = e_{\mu\nu}(q)F_\mathrm{L}(x_\mathrm{B},Q^2) + d_{\mu\nu}(q,p)F_2(x_\mathrm{B},Q^2), \quad (5)$$

where q^μ and p^μ are the photon and hadron momenta,

$$e_{\mu\nu}(q) = g_{\mu\nu} - \frac{q_\mu q_\nu}{q^2} \quad \text{and}$$

$$d_{\mu\nu}(q,p) = -\left[g_{\mu\nu} + 2x_\mathrm{B}\frac{(p_\mu q_\nu + p_\nu q_\mu)}{q^2} + p_\mu p_\nu \frac{4x_\mathrm{B}^2}{q^2}\right],$$

and the $F_k(x_\mathrm{B},Q^2)$(hereafter $k = 2,\mathrm{L}$) are structure functions.

The tensor $F_{\mu\nu}$ is connected via the optical theorem with the amplitude of elastic forward scattering of a photon on a hadron, $T_{\mu\nu}(q,p)$, which may be decomposed in invariant amplitudes $T_k(x_\mathrm{B},Q^2)$ by analogy with (5).

Let us expand the invariant amplitudes in inverse powers of x_B:

$$T_k = \sum_{n=0}^{\infty}\left(\frac{1}{x_\mathrm{B}}\right)^n T_{k,n}. \quad (6)$$

The coefficients $T_{k,n}$ coincide (for even n) with the moments $M_{k,n}$ of the SF F_k:

$$T_{k,n} = M_{k,n} \equiv \int_0^1 \mathrm{d}z z^{n-2}F_k(z,Q^2). \quad (7)$$

2.1 Evaluation of hard SF

We would like to note that the previous formalism can be replicated at the parton level by replacing the hadron momentum p^μ by the gluon one k^μ and the Bjorken variable x_B by the corresponding x. Then the hadron part of the deep inelastic spin-average lepton–parton cross-section can be represented in the form

$$F^p_{\mu\nu} = e_{\mu\nu}(q)F^p_\mathrm{L}(x,Q^2) + d_{\mu\nu}(q,k)F^p_2(x,Q^2), \quad (8)$$

where $F^p_k(x,Q^2)$ are the structure functions of the lepton–parton DIS.

As in our analysis we only consider gluons, the unintegrated gluon distribution into the parton (i.e. into the gluon) $\Phi_g(x,k_\perp^2)$ should have the form

[1] This notation reflects the fact that the structure functions $F^c_{2,\mathrm{L}}$ connect with the functions $C^g_{2,\mathrm{L}}$ in the same form as cross-sections connect with hard ones (see [14–16] and the recent review in [17])

[2] Hereafter we consider only the one-photon exchange approximation

$$\Phi_g(x,k_\perp^2) = \delta(1-x)\hat{\varphi}(k_\perp^2),$$

where $\hat{\varphi}(k_\perp^2)$ is a function of $k_\perp^2$.

The parton SF $F_k^p(x,Q^2)$ and the amplitudes $T_k^p(x,Q^2)$ at the parton level obey equations similar to (6) and (7) with the replacement $x_B \to x$. Then they are connected via the optical theorem:

$$T_k^p(x,Q^2) = \sum_{n=0}^{\infty}\left(\frac{1}{x}\right)^n \int_0^1 \mathrm{d}z z^{n-2} F_k^p(z,Q^2) \quad (n=2m). \tag{9}$$

Thus, the hard SF $C_k^g(x,Q^2,k^2)$ of the parton SF $F_k^p(x,Q^2)$,

$$F_{2,L}^p(x,Q^2) = \int \frac{\mathrm{d}k_\perp^2}{k_\perp^2} C_{2,L}^g(y,Q^2,m_c^2,k_\perp^2)\Theta(x_0-x)\hat{\varphi}(k_\perp^2), \tag{10}$$

can be obtained directly using the amplitudes $T_k^p(x,Q^2)$ at the parton level:

$$T_{2,L}^p(x,Q^2) = \int \frac{\mathrm{d}k_\perp^2}{k_\perp^2} \tilde{C}_{2,L}^g(y,Q^2,m_c^2,k_\perp^2)\hat{\varphi}(k_\perp^2), \tag{11}$$

in the following way:

$$\tilde{C}_k^g(x,Q^2,k^2) = \sum_{n=0}^{\infty}\left(\frac{1}{x}\right)^n \int_0^1 \mathrm{d}z z^{n-2} C_k^g(z,Q^2,k^2)\Theta(z_0-z), \tag{12}$$

where we have extracted a kinematical factor $\Theta(z_0-z)$.

As was already discussed we will work with the gluon part only, keeping non-zero values of the quark masses and the gluon virtuality. The corresponding Feynman diagrams are displayed on Fig. 1. The hard SF $C_k^g(x,Q^2,k^2)$ does not depend on the target type. So it can be calculated in photon–parton DIS and used later in the photon–hadron reaction (see (4)).

2.2 Connection with the Sudakov-like approach

One of the basic ingredients in the Sudakov-like approach is the introduction of an additional light-cone momentum n^μ with $n^2=0$ and $(np)=1$.

The gluon momentum k^μ can be represented by

$$k^\mu = \xi p^\mu + \frac{k^2+k_\perp^2}{2\xi} n^\mu + k_T^\mu, \tag{13}$$

with the following properties:

$$p^2 = n^2 = (pk_T) = (nk_T) = 0, \quad (np)=1, \tag{14}$$

where the 4-vector k_T^μ contains only the transverse part of k^μ, $k_T=(0,k_\perp,0)$, i.e. $k_T^2=-k_\perp^2$ and $\xi = x_B/x$ is the fraction of the proton momentum carried by the gluon (see (4)).

To study the relations between the "usual" approach used here and the Sudakov-like one, it is convenient to introduce the following parametrization for the vector n^μ (see [22]):

$$n^\mu = \frac{2x_B}{Q^2}\left(x_B p^\mu + q^\mu\right). \tag{15}$$

It is easy to check that the properties in (14) are fulfilled.

Then, for the scalar product (kq) we have in the Sudakov-like approach

$$(kq) = \xi(pq) + \frac{k^2+k_\perp^2}{2\xi}(nq) = \frac{Q^2}{2x}\left[1 - x^2\frac{k^2+k_\perp^2}{Q^2}\right]. \tag{16}$$

If $k^2=-k_\perp^2$, then it follows from (16) that

$$x = \frac{Q^2}{2(kq)},$$

which agrees with (2). Also from (13) it follows that

$$k^\mu = x_B p^\mu + k_T^\mu, \tag{17}$$

where x_B is the fraction of the proton momentum carried by the gluon.

2.3 Feynman gauge gluon polarization

As a first approximation we consider gluons having a polarization tensor (hereafter the indices α and β are connected with gluons and μ and ν are connected with photons)[3]

$$\hat{P}^{\alpha\beta} = -g^{\alpha\beta}. \tag{18}$$

This polarization tensor corresponds to the case when gluons do not interact. In some sense the case of polarization is equal to the standard DIS suggestions about parton properties, except for their off-shell property. The polarization in (18) gives the main contribution to the polarization tensor we are interested in (see below):

$$\hat{P}_{BFKL}^{\alpha\beta} = \frac{k_\perp^\alpha k_\perp^\beta}{k_\perp^2} = \frac{x^2}{-k^2} p^\alpha p^\beta, \tag{19}$$

which comes from the high-energy (or k_T-) factorization prescription [14,15,23][4].

[3] In principle, we can use here more general cases of the polarization tensor (for example, the one based on the Landau or unitary gauge). The difference between these and (18) is $\sim k^\alpha$ and/or $\sim k^\beta$ and, hence, it leads to zero contributions because the Feynman diagrams in Fig. 1 are gauge invariant

[4] We would like to note that the BFKL polarization tensor is a particular case of the so-called nonsense polarization of the particles in t-channel making the main contributions for the cross-sections in the s-channel at $s \to \infty$ (see, for example, [24] and references therein). The limit $s \to \infty$ corresponds to small values of the Bjorken variable x_B, which is just the range of our study

Contracting the photon projectors (connected with photon indices of diagrams in Fig. 1),

$$\hat{P}^{(1)}_{\mu\nu} = -\frac{1}{2} g_{\mu\nu} \quad \text{and} \quad \hat{P}^{(2)}_{\mu\nu} = 4x^2 \frac{k_\mu k_\nu}{Q^2},$$

with the hadronic tensor $F_{\mu\nu}$, we obtain the following relations at the parton level (i.e. for off-shell gluons having momentum k_μ):

$$\tilde{\beta}^2 C_2^g(x) = \mathcal{K}\left[f^{(1)} + \frac{3}{2\tilde{\beta}^2} f^{(2)}\right], \tag{20}$$

$$\begin{aligned}\tilde{\beta}^2 C_{\rm L}^g(x) &= \mathcal{K}\left[4bx^2 f^{(1)} + \frac{(1+2bx^2)}{\tilde{\beta}^2} f^{(2)}\right] \\ &= \mathcal{K} f^{(2)} + 4bx^2 \tilde{\beta}^2 C_2^g,\end{aligned} \tag{21}$$

where the normalization factor $\mathcal{K} = e_c^2 \alpha_{\rm s}/(4\pi)x$,

$$P^{(i)}_{\mu\nu} F_{\mu\nu} = \mathcal{K} f^{(i)}, \quad i = 1, 2,$$

and

$$\tilde{\beta}^2 = 1 - 4bx^2,\ b = -k^2/Q^2 \equiv k_\perp^2/Q^2 > 0,\ a = m^2/Q^2,$$

and $\alpha_{\rm s}$ is the QCD coupling constant. The kinematical factor z_0 which appears in (12) is

$$z_0 = \frac{1}{1+4a+b}. \tag{22}$$

Applying the projectors $\hat{P}^{(i)}_{\mu\nu}$ to the Feynman diagrams displayed in Fig. 1, we obtain[5] the following results for the contributions to the expressions:

$$\begin{aligned} f^{(1)} &= -2\beta \\ &\times \Big[1 - (1 - 2x(1+b-2a)[1 - x(1+b+2a)])f_1 \\ &+ (2a-b)(1-2a)x^2 f_2\Big], \end{aligned} \tag{23}$$

$$\begin{aligned} f^{(2)} &= 8x\beta\Big[(1-(1+b)x) \\ &- 2x(bx(1-(1+b)x)(1+b-2a) + a\tilde{\beta}^2)f_1 \\ &+ bx^2(1-(1+b)x)(2a-b)f_2\Big], \end{aligned} \tag{24}$$

where

$$\beta^2 = 1 - \frac{4ax}{(1-(1+b)x)}$$

and[6]

$$f_1 = \frac{1}{\tilde{\beta}\beta} \ln \frac{1+\beta\tilde{\beta}}{1-\beta\tilde{\beta}}, \quad f_2 = \frac{-4}{1-\beta^2\tilde{\beta}^2}.$$

The important regimes, $k^2 = 0$, $m^2 = 0$ and $Q^2 \to 0$, are considered in Appendix C. The $Q^2 = 0$ limit is given in Sect. 2.5.

[5] The contributions of individual scalar components of the diagrams of Fig. 1 (which come after evaluation of the traces of the γ-matrices) are given in Appendix A

[6] We use the variables as defined in [25]

2.4 BFKL-like gluon polarization

Now we take into account the BFKL gluon polarization given in (19). As we already noted in the previous subsection, in these calculations we did not use the Sudakov decomposition and, hence, the hadron momentum p^α is not so convenient to use as variable in our case. Thus, we represent the projector $\hat{P}^{\alpha\beta}_{\rm BFKL}$ as a combination of projectors constructed by the momenta k^α and q^α.

We can represent the tensor $F^{\alpha\beta}$ in the general form:

$$F^{\alpha\beta} = A g^{\alpha\beta} + B q^\alpha q^\beta + C k^\alpha k^\beta + D\left(k^\alpha q^\beta + q^\alpha k^\beta\right), \tag{25}$$

where A, B, C and D are some scalar functions of the variables x, a and b.

From the gauge invariance of the vector current: $k^\alpha F^{\alpha\beta} = k^\beta F^{\alpha\beta} = 0$ we have the following relations:

$$Ck^2 = -\left[A + D(kq)\right], \quad B(kq) = -Dk^2. \tag{26}$$

If we apply the BFKL-like projector $\hat{P}^{\alpha\beta}_{\rm BFKL}$ and use the light-cone properties given in (14), we get the simple relation

$$\hat{P}^{\alpha\beta}_{\rm BFKL} F^{\alpha\beta} = D(kq). \tag{27}$$

The standard projectors $g^{\alpha\beta}$ and $q^\alpha q^\beta$ lead to the relations

$$g^{\alpha\beta} F^{\alpha\beta} = 3A + D\frac{Q^2}{2x}\tilde{\beta}^2, \tag{28}$$

$$4\frac{q^\alpha q^\beta}{Q^2} F^{\alpha\beta} = \frac{\tilde{\beta}^2}{bx^2}\left[A + D\frac{Q^2}{2x}\tilde{\beta}^2\right]. \tag{29}$$

From (28) and (29) we have

$$\left[\left((kq)^2 - k^2q^2\right) g^{\alpha\beta} + 3k^2 q^\alpha q^\beta\right] F^{\alpha\beta} = -D\frac{Q^6}{4x^3}\tilde{\beta}^4, \tag{30}$$

and the BFKL-like projector $\hat{P}^{\alpha\beta}_{\rm BFKL}$ can be represented by

$$\hat{P}^{\alpha\beta}_{\rm BFKL} = -\frac{1}{2}\frac{1}{\tilde{\beta}^4}\left[\tilde{\beta}^2 g^{\alpha\beta} - 12bx^2\frac{q^\alpha q^\beta}{Q^2}\right]. \tag{31}$$

In the previous section we have already calculated the contributions to the hard SF using the first term within the brackets in the r.h.s. of (31). Repeating the above calculations with the projector $\sim q^\alpha q^\beta$, we obtain the total contribution to the hard SF which can be represented as the following shift in the results given in (20)–(24):

$$\begin{aligned} C_2^g(x) &\to C^g_{2,\rm BFKL}(x), \quad C_{\rm L}^g(x) \to C^g_{\rm L,BFKL}(x); \\ f^{(1)} &\to f^{(1)}_{\rm BFKL} = \frac{1}{\tilde{\beta}^4}\left[\tilde{\beta}^2 f^{(1)} - 3bx^2\tilde{f}^{(1)}\right], \\ f^{(2)} &\to f^{(2)}_{\rm BFKL} = \frac{1}{\tilde{\beta}^4}\left[\tilde{\beta}^2 f^{(2)} - 3bx^2\tilde{f}^{(2)}\right], \end{aligned} \tag{32}$$

where

$$\tilde{f}^{(1)} = -\beta\Bigg[\frac{1-x(1+b)}{x} - 2(x(1-x(1+b))(1+b-2a)+a\tilde{\beta}^2)f_1 - x(1-x(1+b))(1-2a)f_2\Bigg], \quad (33)$$

$$\tilde{f}^{(2)} = 4\beta(1-(1+b)x)^2[2-(1+2bx^2)f_1 - bx^2 f_2]. \quad (34)$$

As already has been noted in Sect. 2.3, for the important regimes when $k^2 = 0$, $m^2 = 0$ and $Q^2 \to 0$, the analyses are given in Appendix C.

Notice that our results in (33) and (34) should coincide with the integral representations of [14,16] (at $Q^2 \to 0$ there is full agreement (see the following subsection) with the formulae of [14,16] for the photoproduction of heavy quarks). Our results in (33) and (34) should also agree with those in [26] but a direct comparison is quite difficult because the authors of [26] used a different (and quite complicated) way to obtain their results and the structure of their results is quite cumbersome (see Appendix A in [26]). We have found numerical agreement in the case of $F_2(x_B, Q^2)$ (see Sect. 3 and Fig. 6).

2.5 $Q^2 = 0$ limit

We introduce the new variables $\hat{s}$, ρ and Δ which are useful in the limit $Q^2 \to 0$:

$$\hat{s} = \frac{Q^2}{x},\ \rho = 4ax \equiv \frac{4m^2}{\hat{s}},\ \Delta = bx \equiv \frac{-k^2}{Q^2}x = \frac{k_\perp^2}{\hat{s}}, \quad (35)$$

and express our formulae above as functions of ρ and Δ at asymptotical x values (i.e. small Q^2).

When $x = 0$ we have got the following relations for the intermediate functions:

$$\tilde{\beta}^2 = 1, \quad \beta^2 = 1 - \frac{\rho}{1-\Delta} \equiv \hat{\beta}^2,$$

$$f_1 = \frac{1}{\hat{\beta}}\ln\frac{1+\hat{\beta}}{1-\hat{\beta}} \equiv L(\hat{\beta}), \quad f_2 = \frac{4\hat{\beta}}{\rho}(1-\Delta), \quad (36)$$

$$f^{(1)} = 2\hat{\beta}\Bigg[\left(1+\rho-\frac{\rho^2}{2}\right)L(\hat{\beta}) - (1-\rho) + \left(2+\rho-2L(\hat{\beta})\right)\Delta + 2\left(L(\hat{\beta})-1\right)\Delta^2\Bigg], \quad (37)$$

$$x\tilde{f}^{(1)} = -2\hat{\beta}[2(1-\Delta) - \rho L(\hat{\beta})], \quad f^{(2)} = x\tilde{f}^{(2)} = 0, \quad (38)$$

and thus for the hard SF

$$C_L^g = 0, \quad C_2^g = \mathcal{K} f_{BFKL}^{(1)}, \quad (39)$$

where

$$f_{BFKL}^{(1)} = 2\hat{\beta}\Bigg[\left(1+\rho-\frac{\rho^2}{2}\right)L(\hat{\beta}) - (1+\rho) + \left(8+\rho-(2+3\rho)L(\hat{\beta})\right)\Delta + 2\left(L(\hat{\beta})-4\right)\Delta^2\Bigg]. \quad (40)$$

We note that the results coincide exactly with those from Catani–Ciafaloni–Hautmann work in [14,16] (see (2.2) in [16]) in the case of photoproduction of heavy quarks. The $O(x)$ contribution in the $Q^2 \to 0$ limit is given in Appendix C (see Sect. C.3).

3 Comparison with F_2^c experimental data

With the help of the results obtained in the previous section we analyze the HERA data for SF F_2^c from the ZEUS [3] and H1 [4] Collaborations.

Notice that in [14,16] the $k_\perp^2$-integral has been evaluated using the BFKL results for the Mellin transform of the unintegrated gluon distribution and the Wilson coefficient functions have been calculated analytically for the full perturbative series at asymptotically small x_B values. Since we want to analyze the F_2^c data in a broader range at small x_B, we will use the parameterizations of the unintegrated gluon distribution function (see the following subsection).

3.1 Unintegrated gluon distribution

In this paper we consider four different parameterizations for the unintegrated gluon distribution [18,17]. Two of them [27,28] are presented below and for the others [29, 32] we only describe below some of the most relevant properties.

Firstly, we use the parameterization based on the numerical solution of the BFKL evolution equation [27] (Ryskin–Shabelski (RS) parameterization). The solution has the following form [27]:

$$\Phi(x_B, k^2) = \frac{a_1}{a_2+a_3+a_4} \times \left[a_2 + a_3\frac{Q_0^2}{k^2} + \left(\frac{Q_0^2}{k^2}\right)^2 + \alpha x_B + \frac{\beta}{\epsilon + \ln(1/x_B)}\right] \times C_q\left[\frac{a_5}{a_5+x_B}\right]^{1/2}\left[1 - a_6 x_B^{a_7}\ln\left(k^2/a_8\right)\right] \times (1+a_{11}x_B)(1-x_B)^{a_9+a_{10}\ln(k^2/a_8)}, \quad (41)$$

where

$$C_q = \begin{cases} 1, & \text{if} \quad k^2 < q_0^2(x_B), \\ q_0^2(x_B)/k^2, & \text{if} \quad k^2 > q_0^2(x_B). \end{cases} \quad (42)$$

The parameters ($a_1 - a_{11}, \alpha, \beta$ and ϵ) were found (see [27]) by minimization of the differences between the l.h.s. and the r.h.s. of the BFKL-type equation for the unintegrated gluon distribution $\Phi(x_B, k^2)$ with $Q_0^2 = 4\,\mathrm{GeV}^2$.

Secondly, we also use the results of a BFKL-like parameterization of the unintegrated gluon distribution $\Phi(x_{\rm B}, k_\perp^2, \mu^2)$, according to the J. Blumlein (JB) prescription given in [28]. The proposed method relies upon a straightforward perturbative solution of the BFKL equation where the collinear gluon density $f_g(x_{\rm B}, \mu^2)$ from the standard GRV set [35] is used as the boundary condition in the integral form of (1). Technically, the unintegrated gluon density is calculated as a convolution of the collinear gluon density $f_g(x_{\rm B}, \mu^2)$ with universal weight factor $\mathcal{G}(x, k_\perp^2, \mu^2)$ [28]:

$$\Phi(x_{\rm B}, k_\perp^2, \mu^2) = \int_{x_{\rm B}}^1 \mathcal{G}(\eta, k_\perp^2, \mu^2) f_g\left(\frac{x_{\rm B}}{\eta}, \mu^2\right) \frac{{\rm d}\eta}{\eta}. \quad (43)$$

The universal function $\mathcal{G}(\eta, k_\perp^2, \mu^2)$ can be represented as a series (with some coefficients d_i) $\sum_{i=1} d_i \tilde{I}_{i-1}$, where $\tilde{I}_i = I_i$ if $k_\perp^2 > \mu^2$ and $\tilde{I}_i = J_i$ if $k_\perp^2 < \mu^2$, respectively, and J_i and I_i are Bessel functions for the real and imaginary arguments. The series comes from the expansion of the BFKL anomalous dimensions with respect to the QCD coupling constant $\alpha_{\rm s}$. The first term of the above expansion explicitly describes the BFKL dynamics in the double-logarithmic approximation:

$$\mathcal{G}(\eta, k_\perp^2, \mu^2) = \frac{\bar{\alpha}_{\rm s}}{k_\perp} \begin{cases} J_0(2\sqrt{\bar{\alpha}_{\rm s} \ln(1/\eta) \ln(\mu^2/k_\perp^2)}), \\ \quad \text{if} \quad k_\perp^2 < \mu^2, \\ I_0(2\sqrt{\bar{\alpha}_{\rm s} \ln(1/\eta) \ln(k_\perp^2/\mu^2)}), \\ \quad \text{if} \quad k_\perp^2 > \mu^2, \end{cases} \quad (44)$$

where J_0 and I_0 are the standard for the Bessel functions (of real and imaginary arguments, respectively), and $\bar{\alpha}_{\rm s} = 3\alpha_{\rm s}/\pi$. The parameter $\bar{\alpha}_{\rm s}$ is connected with the pomeron trajectory intercept: $\Delta_P = \bar{\alpha}_{\rm s} 4 \ln 2$ in the LO and $\Delta_P = \bar{\alpha}_{\rm s} 4 \ln 2 - N \bar{\alpha}_{\rm s}^2$ in the NLO approximations. The number N is large: $N \sim 18$ [36–38] and some resummations are needed. Indeed, resummation procedures proposed in the last years lead to a value of $\Delta_P \sim 0.2$–0.3 (see [39,40,17] and references therein).

In our calculations with (43) we use the solution of the LO BFKL equation and consider Δ_P as a free parameter varying from 0.166 to 0.53 with a central value $\Delta_P = 0.35$[7]. We use this value of Δ_P in our present calculations with $\mu^2 = Q_0^2 = 1$ and $4\,{\rm GeV}^2$.

The Kwiecinski–Martin–Stasto (KMS) parameterization [29] is obtained from a unified BFKL and DGLAP description of the SF F_2 data and includes the so-called consistence constraint [30]. The consistence constraint introduces a large correction to the LO BFKL equation. About 70% of the full NLO corrections to the BFKL exponent Δ_P are effectively included in this constraint (see [31]).

The last unintegrated gluon function used here is the one proposed by Golec-Biernat and Wusthoff (GBW) which takes into account saturation effects and has been applied earlier in the analysis of the inclusive and diffractive ep-scattering data [32].

There are several other popular parameterizations (see, for example, those of Kimber–Martin–Ryskin (KMR) [33] and Jung–Salam (JS) [34]), which are not used in our study mostly because of technical difficulties[8]. Note that all above parameterizations give quite similar results except, perhaps, the contributions from the small $k_\perp^2$-range: $k_\perp^2 \leq 1\,{\rm GeV}^2$ (see [17] and references therein). Because we use $Q_0^2 = 4\,{\rm GeV}^2$ in the study of SF $F_{2,{\rm L}}^c$, our results depend very slightly on the small $k_\perp^2$-range of the parameterizations. In the case of JB, GBW and KMS sets this observation is supported below by our results and we expect that the application of the KMR and JS sets should not strongly change our results.

3.2 Numerical results

For the calculation of the SF F_2^c we use (4) in the following form:

$$F_2^c(x_{\rm B}, Q^2) = \int_{x_{\rm B}(1+4a)}^1 \frac{{\rm d}y}{y} C_{2,{\rm BFKL}}^g\left(\frac{x_{\rm B}}{y}, Q^2, 0\right) f_g(y, Q_0^2) + \sum_{i=1}^2 \int_{y_{\rm min}^{(i)}}^{y_{\rm max}^{(i)}} \frac{{\rm d}y}{y} \int_{k_{\perp{\rm min}}^{2(i)}}^{k_{\perp{\rm max}}^{2(i)}} {\rm d}k_\perp^2 \times C_{2,{\rm BFKL}}^g\left(\frac{x_{\rm B}}{y}, Q^2, k_\perp^2\right) \Phi(y, k_\perp^2, \mu^2), \quad (45)$$

where $C_{2,{\rm BFKL}}^g(x_{\rm B}, Q^2, k_\perp^2)$ are given by (32).

The integration limits in (45) have the following values:

$$y_{\rm min}^{(1)} = x_{\rm B}\left(1 + 4a + \frac{Q_0^2}{Q^2}\right), \quad y_{\rm max}^{(1)} = 2x_{\rm B}(1+2a);$$
$$k_{\perp{\rm min}}^{2(1)} = Q_0^2, \quad k_{\perp{\rm max}}^{2(1)} = \left(\frac{y}{x_{\rm B}} - (1+4a)\right) Q^2;$$
$$y_{\rm min}^{(2)} = 2x_{\rm B}(1+2a), \quad y_{\rm max}^{(2)} = 1;$$
$$k_{\perp{\rm min}}^{2(2)} = Q_0^2, \quad k_{\perp{\rm max}}^{2(2)} = Q^2. \quad (46)$$

The ranges of integration correspond to the requirement of positive values in the arguments of the square roots in (23), (24), (33) and (34) and also obey to the kinematical restriction ($z \equiv x_{\rm B}/y) \leq z_0$ with z_0 from (22).

In Figs. 2 and 3 we show the SF F_2^c as a function of $x_{\rm B}$ for different values of Q^2 in comparison with ZEUS [3] and H1 [4] experimental data. For comparison we present the results of the calculation with the different parameterizations for the unintegrated gluon distribution $\Phi(x_{\rm B}, k_\perp^2, Q_0^2)$: the JB, GBW and KMS ones. The differences observed between the curves 2, 3 and 4 are due to the different behavior of the unintegrated gluon distribution as a function of $x_{\rm B}$ and $k_\perp$.

[7] Close values for the parameter Δ_P were obtained, rather, in very different papers (see, for example, [41,42]), in the L3 experiment [43] and by the H1 and ZEUS Collaborations [44]

[8] Note that the RS parameterization [27] is quite old. We use it together with the JB set [28] (when the value $\mu^2 = Q_0^2 = 1\,{\rm GeV}^2$) only once (see Fig. 6) to prove the coincidence between our off-mass-shell matrix elements and those from [26]

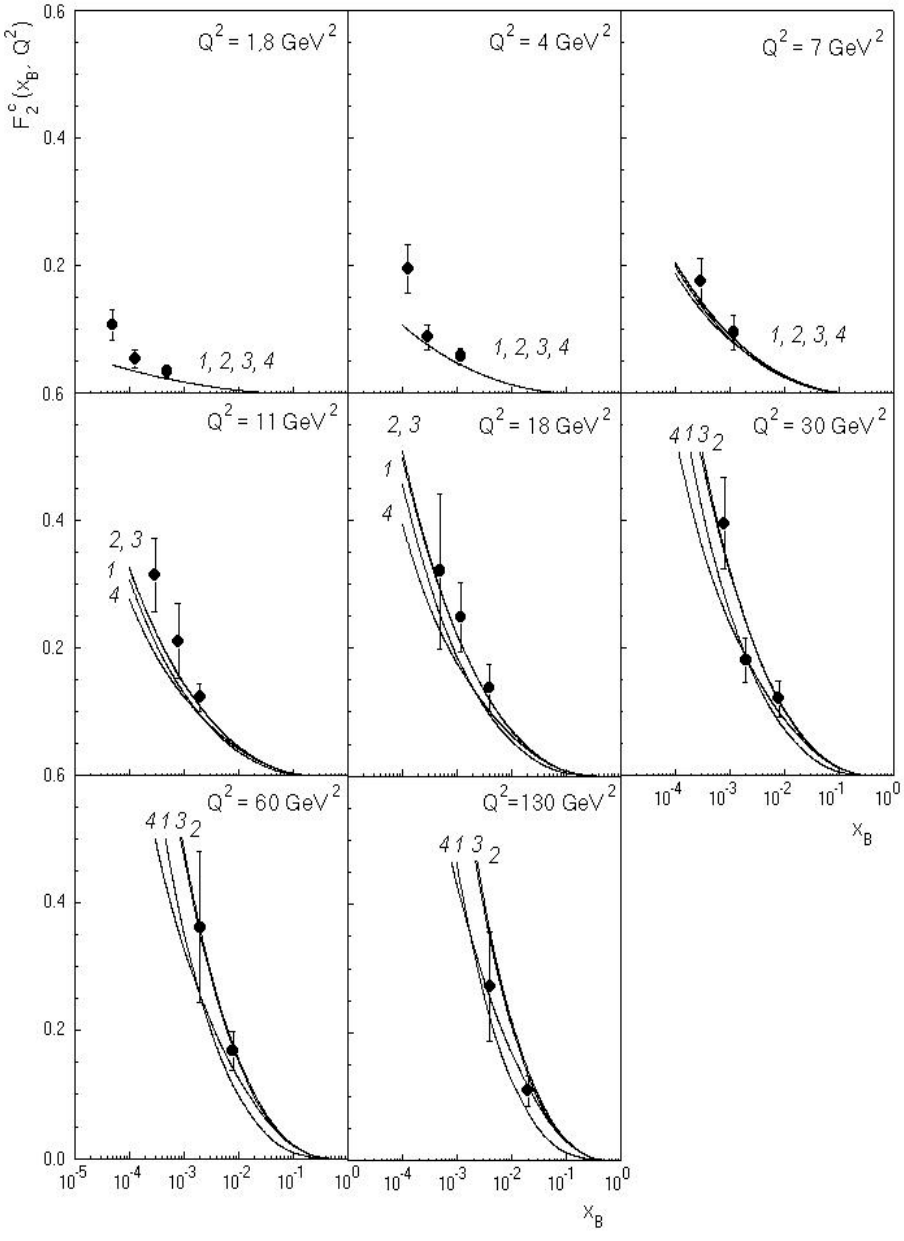

Fig. 2. The structure function $F_2^c(x_B, Q^2)$ as a function of x_B for different values of Q^2 compared to ZEUS data [3]. Curves 1, 2, 3 and 4 correspond to the SF obtained in the standard parton model with the GRV [35] gluon density at the leading order approximation and to SF obtained in the k_T-factorization approach (at $Q_0^2 = 4\,\mathrm{GeV}^2$) with the JB [28], KMS [29] and GBW [32] parameterizations of the unintegrated gluon distribution

We see that at large Q^2 ($Q^2 \geq 10\,\mathrm{GeV}^2$) the F_2^c results obtained in the k_T-factorization approach with KMS and JB parameterizations are close to each other and are higher than the SF obtained in the standard parton model with the GRV gluon density at the LO approximation (see curve 1) and has a more rapid growth in comparison with the standard parton model results, especially at $Q^2 \sim 130\,\mathrm{GeV}^2$ [45]. Otherwise, the k_T-factorization approach with the GBW parameterization is very close to pure QCD predictions: this should be so because the GBW model has deviations from perturbative QCD only at quite low Q^2 values. At $Q^2 \leq 10\,\mathrm{GeV}^2$ the predictions from perturbative QCD (in the GRV approach) and those based on the k_T-factorization approach are very similar[9] and show disagreement with the data below[10] $Q^2 = 7\,\mathrm{GeV}^2$. Unfortunately the available experimental data do not permit one yet to distinguish the k_T-factorization effects from effects due to boundary conditions [27]. Note also that our results for the KMS parameterization are in full agreement with the original results of [33].

For completeness, in Figs. 4 and 5 we present the SF F_2^c as a function of Q^2 for different values of x in comparison with ZEUS [3] and H1 [4] experimental data.

[9] This fact is due to the quite large value of $Q_0^2 = 4\,\mathrm{GeV}^2$ chosen here

[10] A similar disagreement with the data at $Q^2 \leq 2\,\mathrm{GeV}^2$ has been observed for the complete structure function F_2 (see, for example, the discussion in [46] and references therein). We note that the insertion of higher-twist corrections in the framework of the usual perturbative QCD improves the agreement with the data (see [47]) at quite low values of Q^2

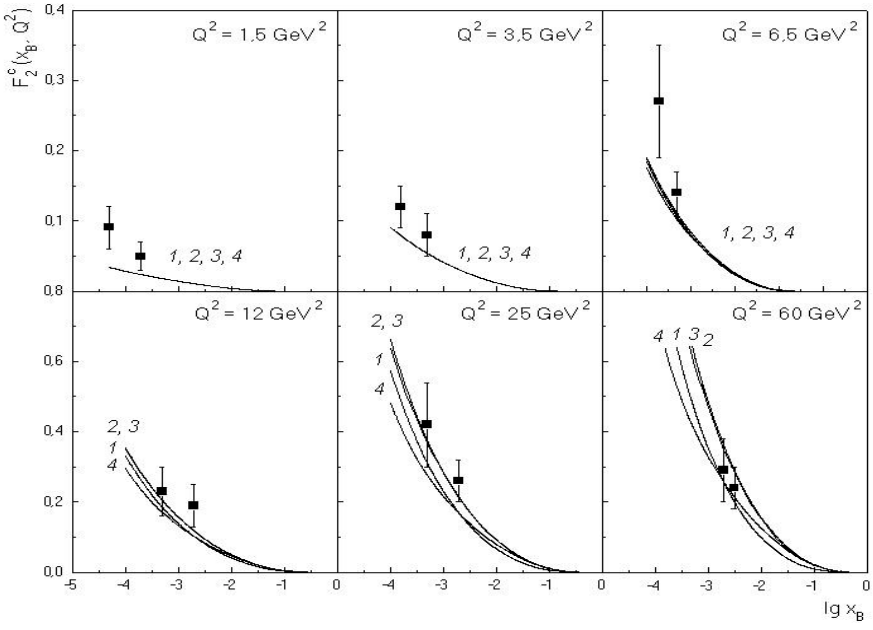

Fig. 3. The structure function $F_2^c(x_B, Q^2)$ as a function of x_B for different values of Q^2 compared to the H1 data [4]. Curves 1, 2, 3 and 4 are as in Fig. 2

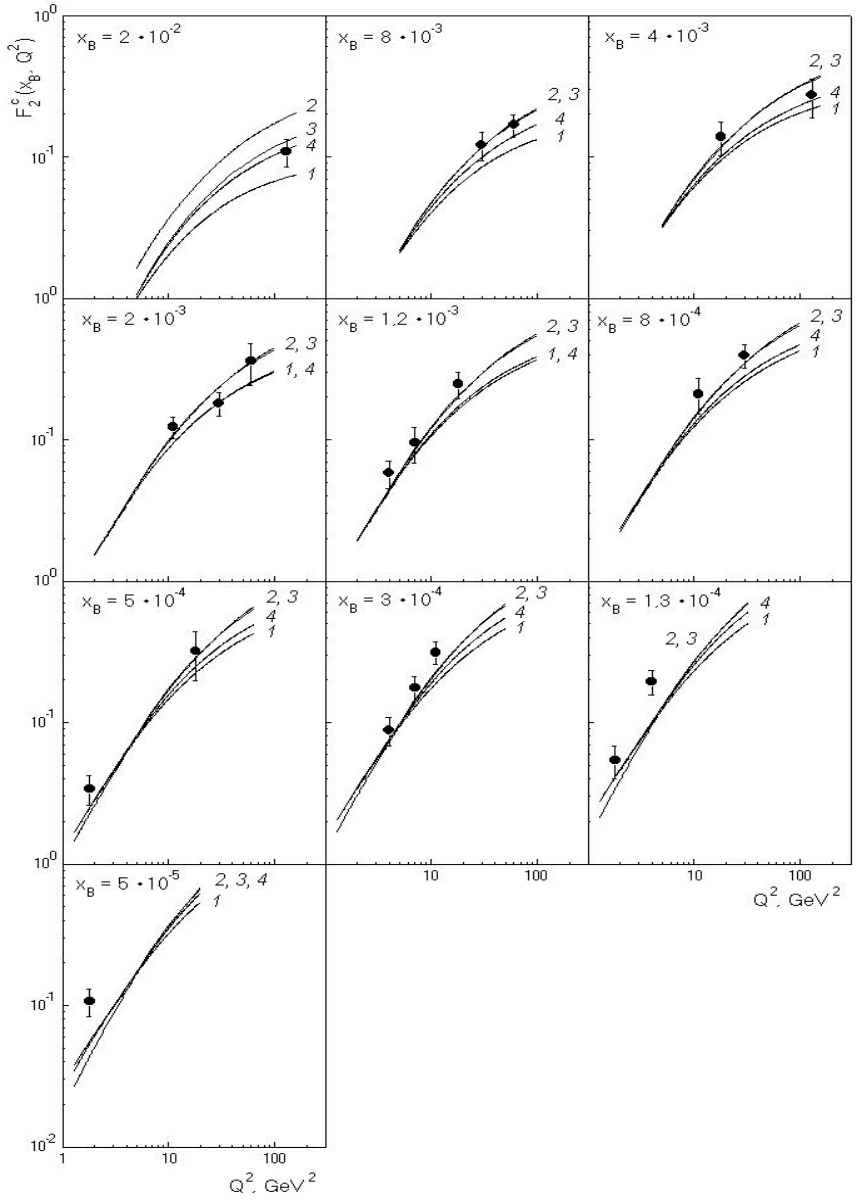

Fig. 4. The structure function $F_2^c(x_B, Q^2)$ as a function of Q^2 for different values of x_B compared to the ZEUS data [3]. Curves 1, 2, 3 and 4 are as in Fig. 2

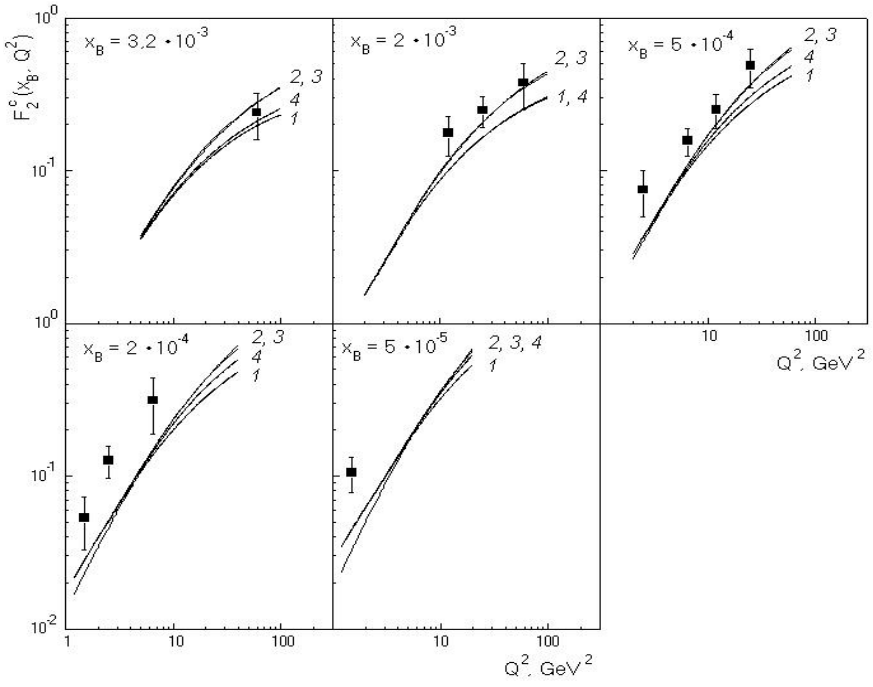

Fig. 5. The structure function $F_2^c(x_B, Q^2)$ as a function of Q^2 for different values of x_B compared to the H1 data [4]. Curves 1, 2, 3 and 4 are as in Fig. 2

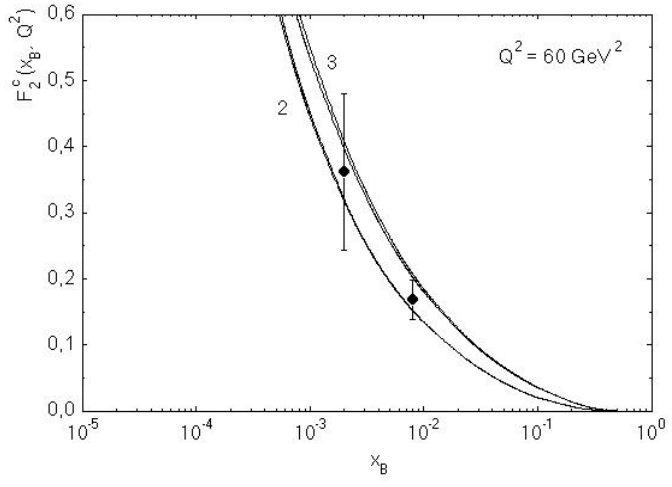

Fig. 6. The structure function $F_2^c(x_B, Q^2)$ as a function of x_B at $Q^2 = 60\,\text{GeV}^2$ compared to the ZEUS data [3]. Curves 2 and 3 correspond to the RS (at $Q_0^2 = 4\,\text{GeV}^2$) [27] and JB (at $Q_0^2 = 1\,\text{GeV}^2$) [28] parameterizations obtained with our off-mass-shell matrix and the ones from [26]

Figure 6 shows the structure function F_2^c at $Q^2 = 60\,\text{GeV}^2$ obtained with two different gluon densities, i.e. the RS (at $Q_0^2 = 4\,\text{GeV}^2$) and JB (at $Q_0^2 = 1\,\text{GeV}^2$) parameterizations. The difference between curves 2 and 3 are mainly due to the different Q_0^2 value used (as we have already shown in Figs. 2 and 3, the difference due to the parameterizations is essentially smaller). So, from Fig. 6 we note that the difference between the k_T-factorization results and those from perturbative QCD increases when we change the value of Q_0^2 in (3) from $4\,\text{GeV}^2$ to $1\,\text{GeV}^2$ [45]. In addition, for each case presented in Fig. 6 we have done the calculations with our off-mass-shell matrix elements and those from [26][11]. The predictions are very similar and cannot be distinguished on curves 2 and 3.

4 Predictions for F_L^c

To calculate the SF F_L^c we have used (45) with the replacement of the hard SF $C_{2,\text{BFKL}}^g$ by $C_{L,\text{BFKL}}^g$, which is given by (32).

In Fig. 7 we show the predictions for F_L^c obtained with different unintegrated gluon distributions. The difference between the results obtained in perturbative QCD and from the k_T-factorization approach is quite similar to the F_2^c case discussed above.

The ratio $R^c = F_L^c/F_2^c$ is shown in Fig. 8. We see $R^c \approx 0.1$–0.3 in a wide region of Q^2. The estimation of R^c is very close to the results for the $R = F_L/(F_2 - F_L)$ ratio (see [48–51]). We would like to note that these values of R^c contradict the suggestion $R^c = 0$ proposed in [3,4]. The effect of R^c on the corresponding differential cross-section should be considered in the extraction of F_2^c from future more precise measurements.

For the ratio R^c we found a quite flat x_B-behavior at low x_B in the low Q^2 region (see Fig. 8), where the approaches based on perturbative QCD and on k_T-factorization give similar predictions (see Figs. 2–5 and 7). It is in agreement with the corresponding behavior of the ratio $R = F_L/(F_2 - F_L)$ (see [48]) at quite large values of Δ_P[12] ($\Delta_P > 0.2$). The low x_B increase of R^c at high

[11] We would like to note that [26] contains several slips: the propagators in (A.1) and the products (pq) in (A.4) and (A.5) should be in the denominator, the indices 2 and L in (A.4) and (A.5) should be transposed

[12] At small values of Δ_P, i.e. when $x^{-\Delta_P} \sim \text{Const}$, the ratio R tends to zero at $x_B \to 0$ (see [52])

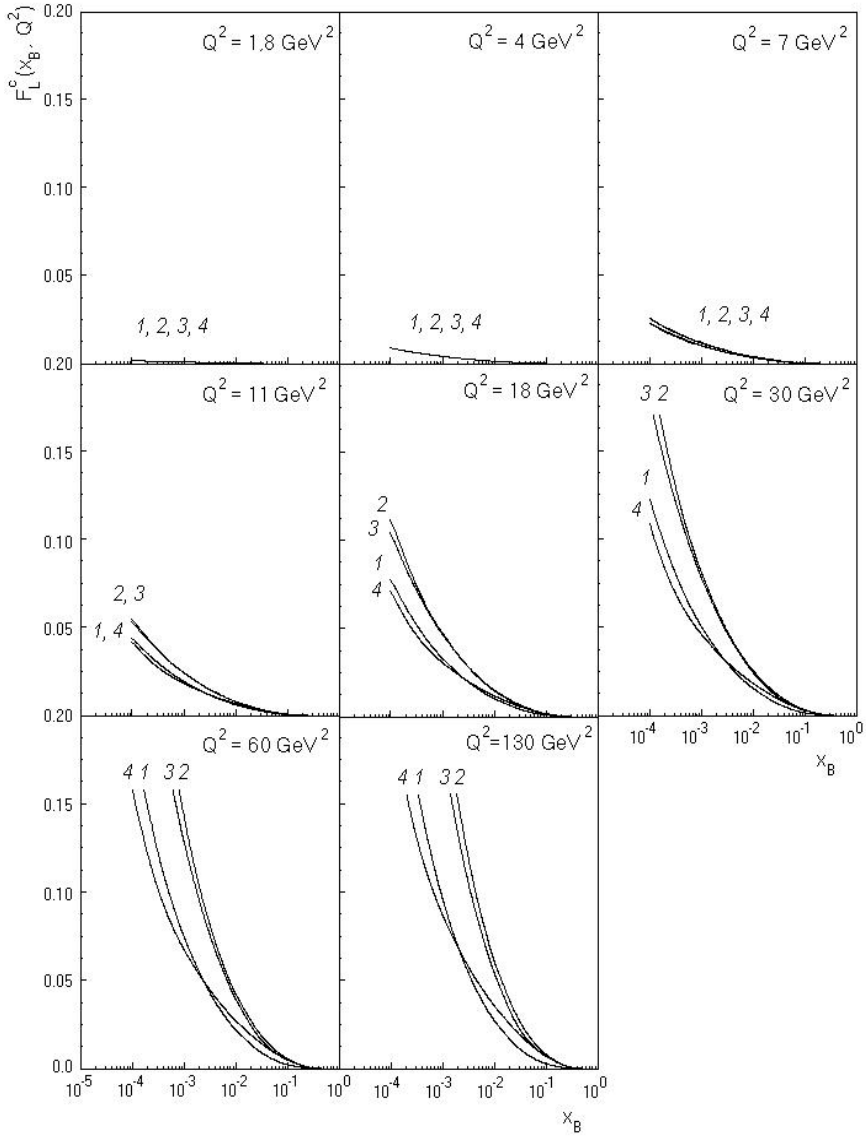

Fig. 7. The structure function $F_L^c(x_B, Q^2)$ as a function of x_B for different values of Q^2. Curves 1, 2, 3 and 4 are as in Fig. 2

Q^2 disagrees with early calculations [48] in the framework of perturbative QCD. This could be due to the small x resummation, which is important at high Q^2 (see Figs. 2–5 and 7). We plan to study in the future this effect on R in the framework of k_T-factorization.

5 Conclusions

We have performed the calculation of the perturbative parts for the structure functions F_2^c and F_L^c for a gluon target having non-zero momentum squared, in the process of photon–gluon fusion. The results have quite a compact form for both: the Feynman gauge and nonsense (or BFKL-like) gluon polarizations.

We have applied the results in the framework of the k_T-factorization approach to the analysis of the present data for the charm contribution to SF F_2 (i.e. for SF F_2^c) and we have given the predictions for F_L^c. The analysis has been performed with several parameterizations of the unintegrated gluon distributions, the JB, GBW and KMS ones, for comparison. We have found good agreement of our results, obtained with these parameterizations of the unintegrated gluon distributions at $Q_0^2 = 4\,\mathrm{GeV}^2$, with the experimental F_2^c HERA data, except at low[13] Q^2 ($Q^2 \leq 7\,\mathrm{GeV}^2$). We have also obtained a quite large contribution of the SF F_L^c at low x_B and high Q^2 ($Q^2 \geq 30\,\mathrm{GeV}^2$). Note that similar results have been obtained also for the RS parameterization [27] (see [53]).

We would like to note the good agreement between our results for F_2^c and the ones obtained in [54] by Monte Carlo studies. Moreover, we have also good agreement with fits of the H1 and ZEUS data for F_2^c (see recent reviews in [55, 17] and references therein) based on perturbative QCD calculations at NLO. But unlike these fits, our analysis uses the universal unintegrated gluon distribution, which

[13] It should be noted that the cross-section of inelastic $c\bar{c}$ and $b\bar{b}$ pair photoproduction at HERA are described by the JB parameterization at a smaller value of Q_0^2 ($Q_0^2 = 1\,\mathrm{GeV}^2$) [18]

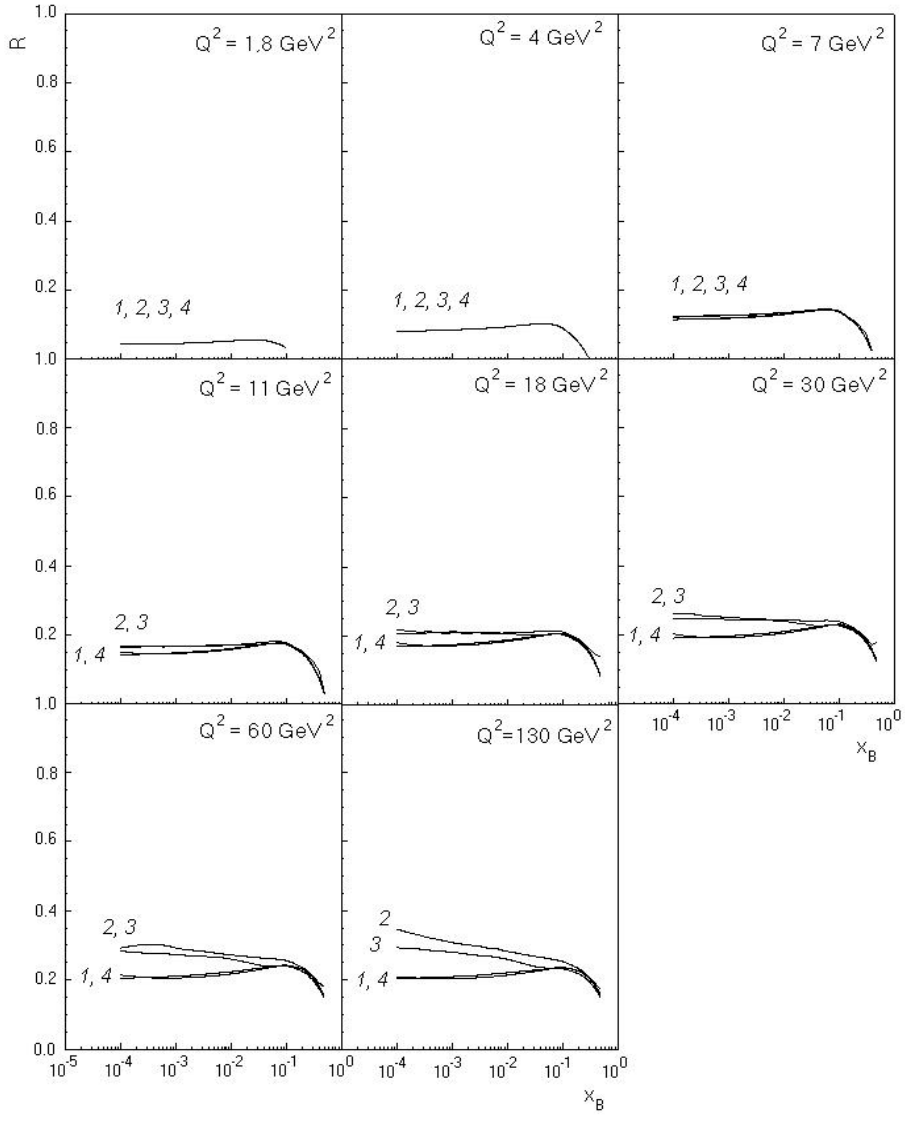

Fig. 8. The ratio $R^c = F_L^c(x_B, Q^2)/F_2^c$ as a function of x_B for different values of Q^2. Curves 1, 2, 3 and 4 are as in Fig. 2

gives in the simplest way the main contribution to the cross-section in the high-energy limit.

It could also be very useful to evaluate the complete F_2 itself and the derivatives of F_2 with respect to the logarithms of $1/x_B$ and Q^2 with our expressions using the unintegrated gluons. We are considering the presentation of this work and also the predictions for F_L in a forthcoming article.

The consideration of the SF F_2 in the framework of the leading-twist approximation of perturbative QCD (i.e. for "pure" perturbative QCD) leads to very good agreement (see [46] and references therein) with HERA data at low x_B and $Q^2 \geq 1.5\,\mathrm{GeV}^2$. The agreement improves at lower Q^2 when higher-twist terms are taken into account [47]. As has been studied in [46,47], the SF F_2 at low Q^2 is sensitive to the small-x_B-behavior of the quark distributions. Thus, the future analysis of F_2 in a broader Q^2-range should require the incorporation of parameterizations for unintegrated quark densities, introduced recently (see [33] and references therein).

The study of the complete SF F_L should also be very interesting. The structure function F_L depends strongly on the gluon distribution (see, for example, [56]), which in turn is determined [57] by the derivative $\mathrm{d}F_2/\mathrm{d}\ln Q^2$. Thus, in the framework of perturbative QCD at low x_B the relation between F_L, F_2 and $\mathrm{d}F_2/\mathrm{d}\ln Q^2$ could be violated by non-perturbative contributions, which are expected to be important in the F_L case (see [58]). The application of the present analysis to F_L will give "non-pure" perturbative QCD predictions for the structure function that should be compared with the data [49,51] and with the "pure" perturbative results of [48].

Acknowledgements. We are grateful to Profs. V.S. Fadin, M. Ciafaloni, I.P. Ginzburg, H. Jung, E.A. Kuraev, L.N. Lipatov and G. Ridolfi for useful discussions. N.P.Z. thanks S.P. Baranov for a careful reading of the manuscript and useful remarks. We thank also the participants of the Workshops Small x phenomenology (Lund, March 2001 and Juni 2002) for the interest in this work and discussions. This study is supported

in part by the RFBR grant 02-02-17513. One of the authors (A.V.K.) was supported in part by Alexander von Humboldt fellowship and INTAS grant N366. G.P. acknowledges the support of Xunta de Galicia (PGIDT00 PX20615PR) and CICyT (AEN99-0589-C02-02). N.P.Z. also acknowledges the support of the Royal Swedish Academy of Sciences.

Appendix A

Here we present the contribution to the amplitude of the DIS process from scalar diagrams[14] in the elastic forward scattering of a photon on a parton. In analogy to (6) one can represent any one-loop diagram of the elastic forward scattering

$$D_{m_1m_2m_3m_4} \equiv \int \frac{\mathrm{d}^D k_1}{(2\pi)^{D/2}} \times d^{m_1}(k_1) d^{m_2}(k-k_1) d^{m_3}(q+k_1) d^{m_4}(q+k_1-k), \tag{A.1}$$

where $d^m(k) = (k^2-m^2)^{-1}$, in the form[15]

$$D_{m_1m_2m_3m_4} = \sum_{n=0}^{\infty} \left(\frac{1}{x}\right)^n \tilde{k}(n) \int_0^{1/(1+4a+b)} \mathrm{d}z z^{n-1} \beta(z) \tilde{f}_{m_1m_2m_3m_4}(z). \tag{A.2}$$

For the application of (A.1) and (A.2) to F_2 and F_L hard SF, only even n are needed. We choose $\tilde{k}(n)$ so that $\tilde{k}(2n) = 1$.

Below we rewrite (A.2) in the symbolic form

$$D_{m_1m_2m_3m_4} \longrightarrow \tilde{k}(n), \quad \tilde{f}_{m_1m_2m_3m_4}(z). \tag{A.3}$$

Then we can represent the needed formulae as follows.

(1) The loops:

$$D_{0110} \longrightarrow \tilde{k}(n) = 1, \quad \tilde{f}_{0110}(z) = 1,$$
$$D_{1001} \longrightarrow \tilde{k}(n) = (-1)^n, \quad \tilde{f}_{1001}(z) = 1. \tag{A.4}$$

(2) The triangles:

$$D_{1110} = D_{0111} \longrightarrow \tilde{k}(n) = 1,$$
$$\tilde{f}_{1110}(z) = \tilde{f}_{0111}(z) = -z f_1(z),$$
$$D_{1011} = D_{1101} \longrightarrow \tilde{k}(n) = (-1)^n,$$
$$\tilde{f}_{1011}(z) = \tilde{f}_{1101}(z) = -z f_1(z). \tag{A.5}$$

(3) The boxes:

$$D_{2110} \longrightarrow \tilde{k}(n) = 1, \quad \tilde{f}_{2110}(z) = -4z^2 f_2(z), \tag{A.6}$$
$$D_{1111} \longrightarrow \tilde{k}(n) = \frac{(1+(-1)^n)}{2}, \quad \tilde{f}_{1111}(z) = 4z^2 f_1(z). \tag{A.7}$$

We would like to note that the result for the second box, D_{1111}, is very similar to the ones for the triangles. In the case of massless quarks this property has been observed in [21,59].

Appendix B

We compare the results obtained in Sect. 2 and Appendix A with well-known formulae obtained in earlier works (see [19,20]).

Following [20] let us consider the kinematics of virtual $\gamma^*\gamma^*$ forward scattering. According to the optical theorem (see Sect. 1) the quantity $F^{\mu\nu\alpha\beta}$ is the absorptive part of the $\gamma^*\gamma^*$ forward amplitude, connected with the cross-section in the usual way. (The expression of the amplitude in terms of the electromagnetic currents is given in Sect. 1.)

In the expansion of $F^{\mu\nu\alpha\beta}$ into invariant functions one should take into account Lorentz invariance, T-invariance (symmetry in the substitution $\mu\nu \leftrightarrow \alpha\beta$) and gauge invariance as well, i.e.[16]

$$q_1^\mu F^{\mu\nu\alpha\beta} = q_1^\nu F^{\mu\nu\alpha\beta} = q_2^\alpha F^{\mu\nu\alpha\beta} = q_2^\beta F^{\mu\nu\alpha\beta}. \tag{B.1}$$

The tensors in which $F^{\mu\nu\alpha\beta}$ is expanded can be constructed in terms of the vectors q_1^μ, q_2^μ and the tensor $g^{\mu\nu}$. In order to explicitly take into account gauge invariance, it is convenient to use their linear combinations:

$$\mathcal{Q}_1^\mu = \sqrt{\frac{-q_1^2}{\mathcal{X}}} \left[q_2^\mu - q_1^\mu \frac{(q_1q_2)}{q_1^2}\right],$$
$$\mathcal{Q}_2^\mu = \sqrt{\frac{-q_2^2}{\mathcal{X}}} \left[q_1^\mu - q_2^\mu \frac{(q_1q_2)}{q_2^2}\right], \tag{B.2}$$
$$R^{\mu\nu} = R^{\nu\mu} = -g^{\mu\nu} + \mathcal{X}^{-1}[(q_1q_2)(q_1^\mu q_2^\nu + q_1^\nu q_2^\mu) - q_1^2 q_2^\mu q_2^\nu - q_2^2 q_1^\mu q_1^\nu], \tag{B.3}$$

where

$$\mathcal{X} = (q_1q_2)^2 - q_1^2 - q_2^2. \tag{B.4}$$

The unit vectors $\mathcal{Q}_i^\mu$ are orthogonal to the vectors q_i^μ and the symmetrical tensor $R^{\mu\nu}$ is orthogonal both to q_1^μ and q_2^μ, i.e. to $\mathcal{Q}_1^\mu$ and $\mathcal{Q}_2^\mu$:

$$q_1^\mu \mathcal{Q}_1^\mu = q_2^\mu \mathcal{Q}_2^\mu = 0, \quad q_i^\mu R^{\mu\nu} = \mathcal{Q}_i^\mu R^{\mu\nu} = 0,$$
$$\mathcal{Q}_1^2 = \mathcal{Q}_1^2 = 1, \quad R^{\mu\nu}R^{\mu\nu} = 2, \quad R^{\mu\nu}R^{\nu\rho} = -R^{\mu\rho}. \tag{B.5}$$

We note that $R^{\mu\nu}$ is a metric tensor of a subspace which is orthogonal to q_1^μ and q_2^μ. In the c.m.s. of the

[14] These diagrams appear after calculation of the traces of the diagrams in Fig. 1

[15] This method is very similar to that in [21,59] in the case of zero quark masses. Usually the consideration of non-zero masses into Feynman integrals strongly complicates the analysis and requires the use of special techniques (see, for example, [60]) to evaluate the diagrams. Here this is not the case, the non-zero quark masses only modify the upper limit of the integral with respect to the Bjorken variable (see the r.h.s. of (A.2))

[16] Sometimes we replace $q \to q_1$ and $k \to q_2$ for the purpose of keeping the symmetry $1 \leftrightarrow 2$ in our formulae in the first part of Appendix B

photons, only two components of $R^{\mu\nu}$ are different from 0 ($R^{xx} = R^{yy} = 1$).

The choice of independent tensors in which the expansion is carried out has a high degree of arbitrariness. We make this choice so that these tensors are orthogonal to each other, and the invariant functions have a simple physical interpretation:

$$\begin{aligned} F^{\mu\nu\alpha\beta} &= R^{\mu\alpha}R^{\nu\beta}F_{\rm TT} + R^{\mu\alpha}\mathcal{Q}_2^\nu\mathcal{Q}_2^\beta F_{\rm TS} + \mathcal{Q}_1^\mu\mathcal{Q}_1^\alpha R^{\nu\beta}F_{\rm ST} \\ &+ \mathcal{Q}_1^\mu\mathcal{Q}_1^\alpha\mathcal{Q}_2^\nu\mathcal{Q}_2^\beta F_{\rm SS} \\ &+ \frac{1}{2}[R^{\mu\nu}R^{\alpha\beta} + R^{\mu\beta}R^{\nu\alpha} - R^{\mu\alpha}R^{\nu\beta}]F_{\rm TT}^\tau \\ &- [R^{\mu\nu}\mathcal{Q}_1^\alpha\mathcal{Q}_2^\beta + R^{\mu\beta}\mathcal{Q}_1^\alpha\mathcal{Q}_2^\nu + (\mu\nu\leftrightarrow\alpha\beta)]F_{\rm TS}^\tau \\ &+ [R^{\mu\nu}R^{\alpha\beta} - R^{\mu\beta}R^{\nu\alpha}]F_{\rm TT}^a \\ &- [R^{\mu\nu}\mathcal{Q}_1^\alpha\mathcal{Q}_2^\beta - R^{\mu\beta}\mathcal{Q}_1^\alpha\mathcal{Q}_2^\nu + (\mu\nu\leftrightarrow\alpha\beta)]F_{\rm TS}^a. \end{aligned} \tag{B.6}$$

The dimensionless invariant functions F_{ab} defined here only depend on the invariants $W^2 = (q_1+q_2)^2$, q_1^2 and q_2^2. The first four functions are expressed through the cross-sections σ_{ab} ($a, b \equiv {\rm S}, {\rm T}$ for scalar and transverse photons, respectively). The amplitudes F_{ab}^τ correspond to transitions with spin-flip for each of the photons with total helicity conservation. The last two amplitudes are antisymmetric.

We would like to represent the results of [19] in terms of our functions, introduced in Sect. 2.

First of all, we return to the variables introduced in Sect. 2. Then we have

$$\mathcal{X} = \frac{Q^4}{4x^2}\tilde\beta^2, \quad \mathcal{Q}_1^\mu = \sqrt{\frac{4bx^2}{Q^2\tilde\beta^2}}\left[q_2^\mu + \frac{1}{2bx}q_1^\mu\right],$$
$$\mathcal{Q}_2^\mu = \sqrt{\frac{4bx^2}{Q^2\tilde\beta^2}}\left[q_1^\mu + \frac{1}{2x}q_2^\mu\right], \tag{B.7}$$

The results of [19] have the form[17]:

$$\begin{aligned} \tilde\beta F_{\rm TT} &= 4x\beta\Big[1 + 4(a-1-b)T + 12bT^2 \\ &- \Big\{1 - 8a^2x^2 + 2\Big(2a - 1 - b \\ &+ 2bx(1-x(1+b))\Big)T + 24b^2T^2\Big\}f_1 + bx^2 f_2\Big], \\ \tilde\beta F_{\rm TS} &= -16x \\ &\times \beta\Big[T - 2x\{ax - b(1+2x(a-1-b))T - 6b^2T^2\}f_1 \\ &+ bx^2(6a - b + 6bT)Tf_2\Big], \\ \tilde\beta F_{\rm ST} &= -16x\beta \\ &\times \Big[T - 2x\{ax - (1+x(2a-1-b))T - 6b^2T^2\}f_1 \\ &+ x^2(6a - b + 6bT)Tf_2\Big], \\ \tilde\beta F_{\rm SS} &= 64bxT^2\beta[2 - (1+2bx^2)f_1 - bx^2 f_2], \\ \tilde\beta F_{\rm TT}^\tau &= 8x\beta \\ &\times \Bigg[2aT + (1-a^2)\frac{x^2}{\tilde\beta^2} + 6bT^2 + x^2\Big\{2(1+a+b) \\ &- b - 2b(2a-1-b)T - 12b^2T^2\Big\}f_1\Bigg], \\ \tilde\beta F_{\rm TS}^\tau &= \tilde\beta F_{\rm ST}^\tau = 16b^{1/2}xT\beta \\ &\times [2x - 3T + x^2\{2a - 1 - b + 6bT\}f_1], \\ \tilde\beta F_{\rm TT}^a &= 4\beta[x - 4T + \{2T - x\}f_1 - bx^3 f_2], \\ \tilde\beta F_{\rm TS}^a &= \tilde\beta F_{\rm ST}^a = -16b^{3/2}x^2T\beta[2f_1 - f_2], \end{aligned}$$

where

$$T = \frac{x(1-x(1+b))}{\tilde\beta^2}.$$

Doing the needed projections on (B.6) we can express the above functions as combinations of $f^{(1)}$, $f^{(2)}$, $\tilde f^{(1)}$ and $\tilde f^{(2)}$ (see Sect. 2). We have

$$\tilde\beta^2 F_{\rm SS} = f^{(1)}, \quad \tilde\beta^2 F_{\rm ST} = \tilde\beta^2 f^{(1)} + \frac{1}{2}f^{(2)}, \tag{B.8}$$
$$\tilde\beta^2 F_{\rm TS} = \frac{1}{2}[\tilde f^{(2)} - f^{(2)}], \quad \tilde\beta^2 F_{\rm TT} = \frac{1}{2}[\tilde\beta^2\tilde f^{(1)} - f^{(1)}].$$

The hard SF calculated in Sect. 2 can be expressed as combinations of F_{AB} ($A, B = {\rm S}, {\rm T}$).

For non-interacting gluons we can write

$$\begin{aligned} \tilde\beta^2 C_2 &= \mathcal{K}[F_{\rm SS} + F_{\rm ST} - 2(F_{\rm TT} + F_{\rm TS})], \\ \tilde\beta^2 C_{\rm L} &= \mathcal{K}[F_{\rm SS} - 2F_{\rm TS} + 4bx^2(F_{\rm ST} - 2F_{\rm TT})]; \end{aligned} \tag{B.9}$$

for the BFKL projector

$$\begin{aligned} \tilde\beta^4 C_{2,{\rm BFKL}} &= \mathcal{K}[F_{\rm SS} + F_{\rm ST} + F_{\rm TS} + F_{\rm TT}], \\ \tilde\beta^4 C_{\rm L,BFKL} &= \mathcal{K}[F_{\rm SS} + F_{\rm TS} + 4bx^2(F_{\rm ST} + F_{\rm TT})]. \end{aligned} \tag{B.10}$$

Appendix C

Here we consider the particular cases of the results obtained in Sect. 2: $k^2 = 0$, $m^2 = 0$ and $Q^2 \to 0$ which are relevant when making comparisons with others.

C.1 The case $k^2 = 0$

When $k^2 = 0$ we have

$$C_2^g(x) = \mathcal{K}\left[f^{(1)} + \frac{3}{2}f^{(2)}\right] \quad \text{and} \quad C_{\rm L}^g(x) = \mathcal{K}f^{(2)}, \tag{C.1}$$

with

$$\begin{aligned} f^{(1)} &= -2\beta\Big[(1 - 2x(1-x)(1-2a)) \\ &\quad - (1 - 2x(1-2a) + 2x^2(1-4a^2))L(\beta)\Big], \end{aligned} \tag{C.2}$$
$$f^{(2)} = 8x\beta[(1-x) - 2xaL(\beta)], \tag{C.3}$$

[17] The original results of [19] contain an additional factor $[-\pi\alpha^2/Q^2]^{-1}$ in comparison with (B.8), that has to do with the different normalization used in our article (see (1)) and in [20]

where

$$\beta^2 = 1 - \frac{4ax}{(1-x)}$$

and the function $L(\beta)$ has been defined in (36).

Equations (C.1)–(C.3) coincide with the results of [61]. Indeed, we have

$$C_2^g = \mathcal{K}(-2)\beta\Big[(1-4x(2-a)(1-x)) - (1-2x(1-2a)+2x^2(1-6a-4a^2))L(\beta)\Big], \quad \text{(C.4)}$$

$$C_{\rm L}^g = \mathcal{K}8x\beta[(1-x)-2xaL(\beta)]. \quad \text{(C.5)}$$

The consideration of the BFKL projector does not change the results given above because the additional terms (see (31)) are proportional to k^2 and they are negligible. The expression in (C.5) also coincides with the corresponding result in [16] (see (A17) and (A18)).

C.2 The case $m^2 = 0$

When $m^2 = 0$ the hard SF $C_k^g(x)$ are defined through $f^{(1)}$ and $f^{(2)}$ (see (20) and (21)) being in this case

$$f^{(1)} = -2[2-(1-2x(1+b)+2x^2(1+b)^2)L(\tilde\beta)], \quad \text{(C.6)}$$

$$f^{(2)} = 8x(1+b)(1-(1+b)x)[1-2bx^2L(\tilde\beta)]. \quad \text{(C.7)}$$

For the hard SF themselves, we have

$$\tilde\beta^4 C_2^g = \mathcal{K}(-2)\,(1-x(1+b)) \times \left[2\left(1-2x(1+b)+\frac{x^2(1-b)^2}{1-x(1+b)}\right) - \Big(1-x(1+b)-4x^3b(1+b) + \frac{x^2(1-b)^2}{1-x(1+b)}\Big)L(\tilde\beta)\right], \quad \text{(C.8)}$$

$$\tilde\beta^4 C_{\rm L}^g = \mathcal{K}8x\,(1-x(1+b)) \times \left[\left((1+b)-2bx\left[1+\frac{x^2(1-b)^2}{1-x(1+b)}\right]\right) + bx\Big(1-3x(1+b)+4x^3b(1+b) + \frac{x^2(1-b)^2}{1-x(1+b)}\Big)L(\tilde\beta)\right]. \quad \text{(C.9)}$$

In the case of the BFKL projector, the hard SF $C_k^g(x)$ are defined by (C.1), (23) and (24) with the replacement $f^{(i)} \to f^{(i)}_{\rm BFKL}$ as in (32). In (32) the expressions for $f^{(i)}$ can be found in (C.6) and (C.7), while for $\tilde f^{(i)}$ they are given by

$$\tilde f^{(1)} = -\frac{(1+b)(1-x(1+b))}{bx}[1-2bx^2L(\tilde\beta)] = -\frac{1}{8bx^2}f^{(2)}, \quad \text{(C.10)}$$

$$\tilde f^{(2)} = 4(1-x(1+b))^2[3-(1+2bx^2)L(\tilde\beta)], \quad \text{(C.11)}$$

and thus

$$f^{(1)}_{\rm BFKL} = C_2^g/\mathcal{K}, \quad \text{(C.12)}$$

$$\tilde\beta^4 f^{(2)}_{\rm BFKL} = 8x(1-x(1+b)) \times \Big[1+b-18bx(1-x(1+b)) + 2bx\left(3-4x(1+b)+6bx^2(1-x(1+b))\right)L(\tilde\beta)\Big]. \quad \text{(C.13)}$$

For the hard SF $C^g_{k,\rm BFKL}(x)$ we have the following results:

$$\tilde\beta^8 C^g_{2,\rm BFKL} = \mathcal{K}(-2)\,(1-x(1+b))\left[2\left(1-5x(1+b) + x^2(1+48b+b^2) + x^3(1+b)(1-48b+b^2) + \frac{x^4(1-b)^4}{1-x(1+b)}\right) - \left(1-x(1+b)+(1-30b+b^2)x^2 + (1-50b+b^2)x^3(1+b) + 72x^4b^2 - 56x^5b^2(1+b) + \frac{x^4(1-b)^4}{1-x(1+b)}\right)L(\tilde\beta)\right], \quad \text{(C.14)}$$

$$\tilde\beta^8 C^g_{\rm L,BFKL} = \mathcal{K}8x\,(1-x(1+b)) \times \left[\left((1+b)-20bx+24b(1+b)x^2 - 2b(1+12b+b^2)x^3 - 2(1+b)b(1-12b+b^2)x^4 - 2bx\frac{x^4(1-b)^4}{1-x(1+b)}\right) + bx\left(7-11x(1+b) + (1-42b+b^2)x^2 + (1-30b+b^2)(1+b)x^3 + 24b^2x^4 - 8b^2(1+b)x^5 + \frac{x^4(1-b)^4}{1-x(1+b)}\right)L(\tilde\beta)\right]. \quad \text{(C.15)}$$

C.3 The case $Q^2 \to 0$

Using the definitions in (35), when $x \to 0$ we have got the following relations (at $O(x)$). For the intermediate functions:

$$\tilde\beta^2 = 1-4x\Delta, \quad \beta^2 = \hat\beta^2(1-4\gamma x),$$

$$f_1 = L(\hat\beta)\,(1+2x(\gamma+\Delta)) - 2x(\gamma+\Delta)\frac{(1-\Delta)}{z},$$

$$f_2 = -\frac{2(1-\Delta)}{z}\left[1-2x\frac{1-\Delta-2z}{z}(\gamma+\Delta)\right], \quad \text{(C.16)}$$

where

$$z = \frac{\rho}{2}, \quad \gamma = \frac{z/2}{(1-\Delta)(1-\Delta-2z)};$$

for the basic functions:

$$
\begin{aligned}
f^{(1)} &= -2\hat{\beta}\Big[1-2(1-\Delta)(\Delta-z)\\
&- (1-2(1-\Delta)\Delta+2(1-z)z)L(\hat{\beta})\\
&+ 2x\Big\{\frac{1-\Delta}{z}\,(\Delta+(\Delta-z)(1-2z\Delta))\\
&- \frac{1-\Delta-z}{z}\gamma \qquad\qquad (C.17)\\
&+ (1-\Delta[3-2(1-\Delta)\Delta+2(1-z)z])L(\hat{\beta})\Big\}\Big],\\
f^{(2)} &= 8x\hat{\beta}\Big[(1-\Delta)\left(1-2\frac{\Delta(1-\Delta)}{z}(z-\Delta)\right)\\
&- (2\Delta^2(1-\Delta)+z(1-2\Delta(1-\Delta)))L(\hat{\beta})\Big],\\
x\tilde{f}^{(1)} &= -\hat{\beta}\Big[\{(1-\Delta)-x(3-6\Delta+4\Delta^2)\}\\
&- \{z+2x(\Delta(1-\Delta)-z)\}L(\hat{\beta})\Big],\\
x\tilde{f}^{(2)} &= 4x\hat{\beta}(1-\Delta)^2[2-L(\hat{\beta})], \qquad (C.18)
\end{aligned}
$$

and thus

$$
\begin{aligned}
f^{(1)}_{\rm BFKL} &= f^{(1)} + 4\hat{\beta}\Delta\Big[3(1-\Delta-zL(\hat{\beta}))\\
&- x\Big\{11-46\Delta+40\Delta^2+4z(1-\Delta) \qquad (C.19)\\
&- 2[1-5(1-\Delta)\Delta+z(5-2z-12\Delta)]\Big\}L(\hat{\beta})\Big],\\
f^{(2)}_{\rm BFKL} &= f^{(2)} - 48x\hat{\beta}\Delta(1-\Delta)[2-L(\hat{\beta})]. \qquad (C.20)
\end{aligned}
$$

Similarly to (C.18), the hard SF in (39) and the functions $f^{(1)}_{\rm BFKL}$ in (40) have the additional terms proportional to x. We have

$$
\begin{aligned}
C_2^g/\mathcal{K} &= f^{(1)} + 4x\hat{\beta}\Big[6\frac{\Delta^2(1-\Delta)^2}{z}+3\\
&- \Delta(11-16\Delta+10\Delta^2+4z(1-\Delta))\\
&+ \{2\Delta[1-5(1-\Delta)\Delta+z(5-2z-3\Delta)]-3z\}\\
&\times L(\hat{\beta})\Big], \qquad (C.21)\\
C_{\rm L}^g/\mathcal{K} &= 8x\hat{\beta}\Big[2\frac{\Delta^2(1-\Delta)^2}{z}\\
&+ 1-2\Delta(2-3\Delta+2\Delta^2+z(1-\Delta)) \qquad (C.22)\\
&+ \{\Delta[1-4(1-\Delta)\Delta+2z(2-z-\Delta)]-z\}L(\hat{\beta})\Big],\\
C^g_{2,\rm BFKL}/\mathcal{K} &= C_2^g/\mathcal{K} + 4\hat{\beta}\Delta\Big[3(1-\Delta-zL(\hat{\beta}))\\
&- x\Big\{47-130\Delta+88\Delta^2+4z(1-\Delta) \qquad (C.23)\\
&- 2[10-23\Delta+14\Delta^2+z(5-2z-18\Delta)]L(\hat{\beta})\Big\}\Big],\\
C^g_{\rm L,BFKL}/\mathcal{K} &= C_{\rm L}^g/\mathcal{K} - 48x\hat{\beta}\Delta[(1-\Delta)(2-3\Delta)\\
&- [(1-\Delta)^2-z\Delta]L(\hat{\beta})]. \qquad (C.24)
\end{aligned}
$$

References

1. H1 Collab., S. Aid et al., Z. Phys. C **72**, 593 (1996); Nucl. Phys. B **545**, 21 (1999)
2. ZEUS Collab., J. Breitweg et al., Phys. Lett. B **407**, 402 (1997)
3. ZEUS Collab., J. Breitweg et al., Eur. Phys. J. C **12**, 35 (2000)
4. H1 Collab., S. Adloff et al., paper submitted to ICHEP2000, Osaka, Japan, Abstract 984
5. EM Collab., J.J. Aubert et al., Nucl. Phys. B **213**, 31 (1983); Phys. Lett. B **94**, 96 (1980); B **110**, 72 (1983)
6. A.M. Cooper-Sarkar, R.C.E. Devenish, A. De Roeck, Int. J. Mod. Phys. A **13**, 3385 (1998)
7. V.N. Gribov, L.N. Lipatov, Sov. J. Nucl. Phys. **15**, 438 (1972); **15**, 675 (1972)
8. L.N. Lipatov, Sov. J. Nucl. Phys. **20**, 94 (1975); G. Altarelli, G. Parisi, Nucl. Phys. B **126**, 298 (1977); Yu.L. Dokshitzer, Sov. Phys. JETP **46**, 641 (1977)
9. B.A. Kniehl et al., Z. Phys. C **76**, 689 (1997); J. Binnewies et al., Z. Phys. C **76**, 677 (1997); M. Cacciari et al., Phys. Rev. D **55**, 2736, 7134 (1997)
10. S. Frixione et al., Phys. Lett. B **348**, 653 (1995); Nucl. Phys. B **454**, 3 (1995)
11. M.A.G. Aivazis et al., Phys. Rev. D **50**, 3102 (1994)
12. L.N. Lipatov, Sov. J. Nucl. Phys. **23**, 338 (1976); E.A. Kuraev, L.N. Lipatov, V.S. Fadin, Sov. Phys. JETP 44 (1976) **443**; **45**, 199 (1977); Ya.Ya. Balitzki, L.N. Lipatov, Sov. J. Nucl. Phys. **28**, 822 (1978); L.N. Lipatov, Sov. Phys. JETP **63**, 904 (1986)
13. J. Kwiecinski, Acta Phys. Polon. B **27**, 3455 (1996)
14. S. Catani, M. Ciafaloni, F. Hautmann, Phys. Lett. B **242**, 97 (1990); Nucl. Phys. B **366**, 135 (1991)
15. J.C. Collins, R.K. Ellis, Nucl. Phys. B **360**, 3 (1991)
16. S. Catani, M. Ciafaloni, F. Hautmann, preprint CERN - TH.6398/92, in Proceeding of the Workshop on Physics at HERA (Hamburg, 1991), v.2, p. 690; S. Catani, preprint DFF 254-7-96 (hep-ph/9608310)
17. Bo Andersson et al., hep-ph/0204115
18. A.V. Lipatov, N.P. Zotov, Mod. Phys. Lett. A **15**, 695 (2000); A.V. Lipatov, V.A. Saleev, N.P. Zotov, Mod. Phys. Lett. A **15**, 1727 (2000)
19. V.N. Baier, V.S. Fadin, V.A. Khose, Zh. Eksp.Teor. Fiz. **50**, 156 (1966) [Sov. J. JETP **23**, 104 (1966)]; V.N. Baier, V.M. Katkov, V.S. Fadin, Relativistic electron radiation (Atomizdat, Moscow 1973) (in Russian); V.G. Zima, Yad. Fiz. **16**, 1051 (1972) [Sov. J. Nucl. Phys. **16**, 580 (1973)]
20. V.M. Budnev, I.F. Ginsburg, G.V. Meledin, V.G. Serbo, Phys. Rept. **15**, 181 (1975)
21. D.I. Kazakov, A.V. Kotikov, Theor. Math. Phys. **73**, 1264 (1987); Nucl. Phys. B **307**, 721 (1988); E B **345**, 299 (1990)
22. R.K. Ellis, W. Furmanski, R. Petronzio, Nucl. Phys. B **207**, 1 (1982); B **212**, 29 (1983)
23. E.M. Levin, M.G. Ryskin, Yu.M. Shabelskii, A.G. Shuvaev, Sov. J. Nucl. Phys. **53**, 657 (1991)

24. E.A. Kuraev, L.N. Lipatov, Yad. Fiz. **16**, 1060 (1972) [Sov. J. Nucl. Phys. **16**, 584 (1973)]
25. W. Vogelsang, Z. Phys. C **50**, 275 (1991); A. Gabrieli, G. Ridolfi, Phys. Lett. B **417**, 369 (1998)
26. G. Bottazzi, G. Marchesini, G.P. Salam, M. Scorletti, JHEP **9812**, 011 (1998)
27. M.G. Ryskin, Yu.M. Shabelski, Z. Phys. C **61**, 517 (1994); C **66**, 151 (1995)
28. J. Blumlein, preprint DESY 95-121 (hep-ph/9506403)
29. J. Kwiecinski, A.D. Martin, A.M. Stasto, Phys. Rev. D **56**, 3991 (1997)
30. J. Kwiecinski, A.D. Martin, P.J. Sutton, Phys. Rev. D **52**, 1445 (1995); Z. Phys. C **71**, 585 (1996)
31. J. Kwiecinski, A.D. Martin, J.J. Outhwaite, Eur. Phys. J. C **9**, 611 (1999)
32. K. Golec-Biernat, M. Wusthoff, Phys. Rev. D **59**, 014017 (1999); D **60**, 014015, 114023 (1999)
33. M.A. Kimber, A.D. Martin, M.G. Ryskin, Phys. Rev. D **63**, 114027 (2001)
34. H. Jung, G. Salam, Eur. Phys. J. C **19**, 351 (2001); H. Jung, hep-ph/9908497
35. M. Gluck, E. Reya, A. Vogt, Z. Phys. C **67**, 433 (1995)
36. V.N. Fadin, L.N. Lipatov, Phys. Lett. B **429**, 127 (1998); M. Ciafaloni, G. Camici, Phys. Lett. B **430**, 349 (1998)
37. A.V. Kotikov, L.N. Lipatov, Nucl. Phys. B **582**, 19 (2000), in Proceedings of the XXXV Winter School, Repino, S'Peterburg, 2001 (hep-ph/0112346; hep-ph/0208220)
38. D.A. Ross, Phys. Lett. B **431**, 161 (1998)
39. G. Salam. JHEP **9807**, 019 (1998); Acta Phys. Polon. B **30**, 3679 (1999)
40. S.J. Brodsky, V.S. Fadin, V.T. Kim, L.N. Lipatov, G.B. Pivovarov, JETP Lett. **70**, 155 (1999)
41. N.N. Nikolaev, B.G. Zakharov, Phys. Lett. B **333**, 250 (1994); Phys. Lett. B **327**, 157 (1994); J. Kwiecinski, A.D. Martin, P.J. Sutton, Z. Phys. C **71**, 585 (1996); B. Andersson, G. Gustafson, H. Kharrazina, J. Samuelsson, Z. Phys. C **71**, 613 (1996); N.N. Nikolaev, V.R. Zoller, in Proceedings QCD-2000, Villefranche-sur-Mer, January 2000 (hep-ph/0001084); B.I. Ermolaev, M. Greco, S.I. Troyan, Nucl. Phys. B **594**, 71 (2001); A.B. Kaidalov, Talk presented at the XXXV Winter School, Repino, S'Peterburg, February 2001 (hep-ph/0103011); A.V. Kotikov, G. Parente, preprint US-FT/3-02 (hep-ph/0207276)
42. S.P. Baranov, N.P. Zotov, Phys. Lett. B **458**, 389 (1999)
43. L3 Collaboration, M. Acciarri et al., Phys. Lett. B **453**, 333 (1999); M. Kienzle, talk given at the International Symposium on Evolution Equations and Large Order Estimates in QCD, Gatchina, Russia, May, 2000
44. H1 Collaboration, C. Adloff et al., Phys. Lett. B **520**, 183 (2001); B. Surrow, talk given at the International Europhysics Conference on High Energy Physics, July 2001 (hep-ph/0201025)
45. A.V. Lipatov, N.P. Zotov, in Proceedings of the 8th International Workshop on Deep Inelastic Scattering, DIS 2000 (2000) (World Scientific), p. 157
46. A.V. Kotikov, G. Parente, Nucl. Phys. B **549**, 242 (1999); Nucl. Phys. (Proc. Suppl.) **99A**, 196 (2001); in Proceedings of the International Conference PQFT98 (1998), Dubna (hep-ph/9810223); in Proceedings of the 8th International Workshop on Deep Inelastic Scattering, DIS 2000 (2000), Liverpool, p. 198 (hep-ph/0006197)
47. A.V. Kotikov, G. Parente, in Proceedings International Seminar Relativistic Nuclear Physics and Quantum Chromodynamics (2000), Dubna (hep-ph/0012299); in Proceedings of the 9th International Workshop on Deep Inelastic Scattering, DIS 2001 (2001), Bologna (hep-ph/0106175)
48. A.V. Kotikov, JETP **80**, 979 (1995); A.V. Kotikov, G. Parente, in Proceedings International Workshop on Deep Inelastic Scattering and Related Phenomena (1996), Rome, p. 237 (hep-ph/9608409); Mod. Phys. Lett. A **12**, 963 (1997); JETP **85**, 17 (1997); hep-ph/9609439
49. H1 Collab., S. Aid et al., Phys. Lett. B **393**, 452 (1997); H1 Collab., D. Eckstein, in Proceedings International Workshop on Deep Inelastic Scattering (2001), Bologna; H1 Collab., M. Klein, in Proceedings of the 9th International Workshop on Deep Inelastic Scattering, DIS 2001 (2001), Bologna
50. R.S. Thorne, Phys. Lett. B **418**, 371 (1998)
51. CCFR/NuTeV Collab., U.K. Yang et al., in Proceedings International Conference on High Energy Physics (2000) Osaka, Japan (hep-ex/0010001); CCFR/NuTeV Collab., A. Bodek, in Proceedings of the 9th International Workshop on Deep Inelastic Scattering, DIS 2001 (2001), Bologna (hep-ex/00105067)
52. S. Keller, M. Miramontes, G. Parente, J. Sánchez-Guillén, O.A. Sampayo, Phys. Lett. B **270**, 61 (1990); L.H. Orr, W.J. Stirling, Phys. Rev.Lett. B **66**, 1673 (1991); E. Berger, R. Meng, Phys. Lett. B **304**, 318 (1993); A.V. Kotikov, JETP Lett. **59**, 1 (1994); Phys. Lett. B **338**, 349 (1994)
53. A.V. Kotikov, A.V. Lipatov, G. Parente, N.P. Zotov, in Proceedings of the XVIth International Workshop High Energy Physics and Quantum Field Theory (2001), Moscow (hep-ph/0208195); in Proceedings of the International School Heavy Quark Physics (2002), Dubna
54. H. Jung, Nucl. Phys. (Proc. Suppl.) **79**, 429 (1999)
55. G. Wolf, preprint DESY 01-058 (hep-ex/0105055); L. Gladilin, I. Redoldo, to appear in The THERA Book (hep-ph/0105126)
56. A.M. Cooper-Sarkar, G. Ingelman, R.G. Roberts, D.H. Saxon, Z. Phys. C **39**, 281 (1988); A.V. Kotikov, Phys. Atom. Nucl. **57**, 133 (1994); Phys. Rev. D **49**, 5746 (1994)
57. K. Prytz, Phys. Lett. B **311**, 286 (1993); A.V. Kotikov, JETP Lett. **59**, 667 (1994); A.V. Kotikov, G. Parente, Phys. Lett. B **379**, 195 (1996)
58. J. Bartels, K. Golec-Biernat, K. Peters, Eur. Phys. J. C **17**, 121 (2000)
59. A.V. Kotikov, Theor. Math. Phys. **78**, 134 (1989)
60. A.V. Kotikov, Phys. Lett. B **254**, 158 (1991); B **259**, 314 (1991); B **267**, 123 (1991)
61. E. Witten, Nucl. Phys. B **104**, 445 (1976); M. Gluck, E. Reya, Phys. Lett. B **83**, 98 (1979); F.M. Steffens, W. Melnitchouk, A.W. Thomas, Eur. Phys. J. C **11**, 673 (1999)
62. A.V. Kotikov, A.V. Lipatov, N.P. Zotov (hep-ph/0207226)

Note added in proof. During the completion of this article the study of the complete structure function F_L discussed in Conclusion has been done in [62] in the framework of k_T-factorization.